Synthesis of colloidal suspensions of CoOx/C nanomaterials using laser ablation of solids in liquids

N. E.-Sánchez[a,f,*], A. R. Vilchis-Nestor[b], M. A. Camacho-López[c], S. Camacho-López[d], M. C. González[e], and M. Camacho-López[f,**]

[a]*Doctorado en Ciencia de Materiales de la Facultad de Química, Universidad Autónoma del Estado de México, Paseo Colón Esquina Paseo Tollocan S/N, Toluca Estado de México, México, 50120.*
[b]*Centro Conjunto de Investigación en Química Sustentable, UAEM-UNAM. Facultad de Química, Universidad Autónoma del Estado de México. Toluca, 50200. México.*
[c]*Laboratorio de Fotomedicina, Biofotónica y Espectroscopía Láser de Pulsos Ultracortos, Facultad de Medicina, Universidad Autónoma del Estado de México, Jesús Carranza y Paseo Tollocan S/N, Toluca, 50120, México.*
[d]*Departamento de óptica, Centro de Investigación Científica y de Educación Superior de Ensenada, Carretera Ensenada-Tijuana, No. 3918, Zona Playitas, Ensenada B.C., 22860, México.*
[e]*TecNM/Tecnológico de Estudios Superiores de Jocotitlán, Carretera Toluca Atlacomulco Km 44.8, Ejido de San Juan y San Agustín, Jocotitlán 50700, México.*
[f]*Laboratorio de Investigación y Desarrollo de Materiales Avanzados, Facultad de Química, Universidad Autónoma del Estado de México, Campus Rosedal, Km 14.5 Carretera Toluca-Atlacomulco, Toluca, 50200, México.*
*email:*nenriquezs682@alumno.uaemex.mx, **macamacholo@uaemex.mx*

Received 12 January 2026; accepted 11 March 2026

In this work, colloidal suspensions of CoOx/C nanomaterials were synthesized using laser ablation of solids in liquids. In the first stage, experiments were carried out using a cobalt target and deionized water as the liquid medium in order to establish the conditions for the synthesis of the nanomaterials. Subsequently, the cobalt target was irradiated in two liquid media containing carbon nanomaterials: a colloidal suspension of carbon nanoparticles (CNPs) and another of graphene oxide nanosheets (GONs). The effect of the liquid medium was studied as an important parameter, which determines the composition and structure of the final products. The resulting CoOx/C nanomaterials were characterized morphologically and structurally using infrared spectroscopy, Raman spectroscopy, and transmission electron microscopy. In addition, the optical properties of the colloidal suspensions were evaluated using fluorescence spectroscopy. The results show that ablation in deionized water produces Co_3O_4 nanoparticles with an average diameter of 10.43 nm, while ablation in colloidal suspensions of carbon nanomaterials led to the formation of two types of structures: carbon-coated CoOx nanoparticles and spherical CoOx nanoparticles embedded in a carbon matrix. These cobalt oxide and carbon-based nanomaterials have broad potential in biomedical applications and energy storage devices.

Keywords: Laser ablation; photoluminescence; carbon nanostructures; cobalt oxides; CoOx/C nanomaterials.

DOI: https://doi.org/10.31349/RevMexFis.72.041004

1. Introduction

Nanoscale cobalt oxides have attracted considerable interest due to their catalytic, electrochemical, and optical properties, making them attractive candidates for applications ranging from sensors and heterogeneous catalysis to energy storage devices and biomedicine [1-3]. However, their efficiency can be limited by low intrinsic conductivity and the tendency of nanoparticles to agglomerate. A common strategy to reduce these limitations is to combine them with carbon nanomaterials, which provide greater stability, conductivity, and a suitable surface for dispersing and protecting the particles. This combination can result in nanocomposites with synergistic properties, reflected in more efficient charge transfer, greater structural stability, and improved optical or electrochemical behavior. Nanomaterials based on metal oxides and carbon combine the functionality of metal oxide with the conductivity and structural stability of carbon. As a result, CoOx/C nanocomposites have been established as attractive candidates for applications in supercapacitors, catalysis, controlled drug delivery, and bioimaging platforms [4-6].

Laser-assisted synthesis has become established as a powerful tool for the production of advanced nanomaterials. In particular, laser ablation of solids in liquids (LASL) enables the design of nanomaterials with unique properties compared to those obtained through conventional synthesis routes. This technique is considered low cost, as both the solid targets and the solvents used are generally cheaper than the salts or metal precursors used in traditional chemical methods. In addition to its accessibility, LASL is a highly versatile methodology capable of generating high-purity nanoparticles by irradiating a solid target immersed in a liquid medium. The possibility of combining different targets and solvents facilitates the synthesis of a wide

range of materials, including metal nanoparticles, oxides, alloys, carbides, among others [7-9]. Likewise, when the liquid medium contains preformed carbon nanomaterials, the technique enables the direct formation of nanocomposites [10,11], further expanding its potential for design and functionalization.

Nanoparticles of cobalt and its oxides have been synthesized using laser ablation and fragmentation techniques in liquids. In particular, laser fragmentation of Co [12,13], CoO [12], Co_3O_4 [12,14,15], and Co_2O_3 [16] powders dispersed in deionized water has resulted in the production of CoO [15], Co_3O_4 [12-15], and Co_2O_3 [16] nanoparticles. Similarly, laser ablation of a solid Co target in deionized water produced Co_3O_4 nanoparticles [17,18]. When organic solvents such as toluene or acetone are used as the liquid medium, it is possible to synthesize core-shell nanoparticles of Co@C [19] and Co_3C@C [20]. In all these studies, the synthesis parameters vary widely, with wavelengths between 355 and 1064 nm, irradiation times from 10 to 60 min, and energies ranging from 30 mJ to 20 J. As can be seen, there are few reports on the synthesis of nanocomposites and core-shell structures of cobalt and carbon, since the synthesis has been carried out mainly in water as the liquid medium.

In this work, colloidal suspensions of CoOx/C nanomaterials were synthesized using LASL. In the first stage, the cobalt target was irradiated using deionized water as the liquid medium to establish the conditions for the synthesis of the nanomaterials. Subsequently, two liquid media containing carbon nanomaterials were used: a colloidal suspension of carbon nanoparticles (CNPs) and another of graphene oxide nanosheets (GONs). The influence of the ablation medium on the morphology, structure, and optical properties of the resulting nanomaterials was evaluated using infrared spectroscopy, Raman spectroscopy, transmission electron microscopy, and fluorescence spectroscopy. The results indicate that ablation in deionized water produces Co_3O_4 nanoparticles, while ablation in colloidal suspensions of carbon nanomaterials generates two types of structures: carbon-coated CoOx nanoparticles and spherical CoOx nanoparticles embedded in a carbon matrix. These results reveal how the liquid medium modulates the formation of CoOx nanoparticles, providing important information for designing nanomaterials with potential applications in biomedicine and energy storage.

2. Experimental

2.1. Synthesis

Colloidal suspensions of CoOx/C nanomaterials were obtained using the LASL technique. In a first stage, the synthesis conditions were established using a cobalt target and deionized water as the liquid medium. The experiments were carried out as illustrated in Fig. 1a), a cobalt target (2.54 cm in diameter $\times$ 0.40 cm thick, 99.95% purity, Kurt J. Lesker Company) was immersed in 20 ml of deionized water (Wöhler), using a 50 ml glass vessel forming an optical path of 1.9 cm. The cobalt target was irradiated for 30 min using a pulsed Nd:YAG laser (Surelite, Continuum) with an emission wavelength of 1064 nm and a repetition rate of 20 Hz; the target was constantly moved to avoid irradiation in the same place. To focus the laser pulses (105 mJ), a lens was placed 9.6 cm from the target, forming a 1 mm diameter spot on the surface of the target, giving a per pulse laser fluence of 13.37 J/cm^2.

Subsequently, the cobalt target was irradiated in two liquid media containing carbon nanomaterials: a colloidal suspension of CNPs and another of GONs. The suspensions were previously obtained by ultrasonic irradiation of coffee biochar dispersed in toluene and hydrogen peroxide. The synthesis and characterization of these materials has already been reported by our research group previously [21]. The liquid media were prepared as follows. For the colloidal suspension of CNPs, 3.5 ml of the colloidal suspension in toluene was diluted in 16.5 ml of isopropyl alcohol (Trademark). To prevent oxidation of the cobalt target, the colloidal suspension of GONs in hydrogen peroxide was dehydrated at 75 °C using a hot plate, and a solution was then prepared by placing 4.63 mg of the dehydrated material in 20 ml of deionized water (Wöhler).

Figure 1b) shows a photograph of the colloidal suspension of cobalt oxide nanoparticles obtained using deionized water as the liquid medium, which has a brown color. Figures 1c) and 1d) show photographs of the colloidal suspensions of CoOx/C nanomaterials obtained using the colloidal

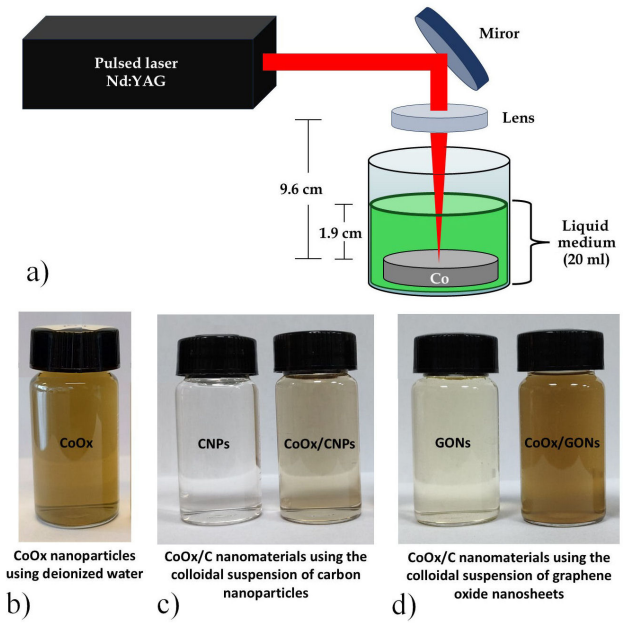

FIGURE 1. a) Experimental diagram used for the synthesis of colloidal suspensions of CoOx/C nanomaterials. b) Cobalt oxide nanoparticles obtained using deionized water as the liquid medium. CoOx/C nanomaterials obtained using c) the colloidal suspension of CNPs and d) the colloidal suspension of GONs as the liquid medium, respectively.

suspension of CNPs and the colloidal suspension of GONs, respectively. For comparison purposes, the liquid media are shown in the image. We can see that the colloidal suspensions obtained from the ablation process have a brown hue compared to the liquid media used, which have a translucent hue (colloidal suspension of CNPs) and a yellowish hue (colloidal suspension of GONs).

2.2. Characterization

CoOx nanoparticles were characterized using Raman spectroscopy and transmission electron microscopy (TEM). Whereas CoOx/C nanomaterials were characterized morphologically and structurally using infrared spectroscopy (FTIR), Raman spectroscopy, and TEM. In addition, the optical properties of the colloidal suspensions of CoOx/C nanomaterials were characterized by fluorescence spectroscopy.

Raman characterization was performed with a Raman spectrometer (Xplora Plus, Jobin-Yvon-Horiba) using a green laser (λ = 532 nm) with a power of 2.5 mW. A 50X objective lens was used to focus the laser beam on the sample.

FTIR spectra were taken on an IR spectrometer (IRPrestige-21, Shimadzu) from 550 to 4000 cm^{-1} for the liquid media (CNPs and GONs) and the colloidal suspensions of CoOx/C nanomaterials. For the analyses, part of the colloidal suspension was dripped onto a microscope slide and the liquid medium was evaporated at 70 °C using a hot plate.

The morphological and structural characterization of the nanomaterials was performed using a transmission electron microscope (JEOL 2100) with an acceleration voltage of 200 kV. Image acquisition was performed on samples prepared by evaporation at room temperature of a drop of the colloidal suspension on a grid.

The photoluminescence emission spectra were obtained using a spectrophotometer (Fluoromax-p, Jobin-Yvon-Horiba) with an excitation wavelength of 370 nm. The spectra were obtained by placing 3.5 ml of the diluted colloidal suspension in a quartz cuvette with an optical path length of 10 mm. The dilution was performed by placing 3 ml of the colloidal suspension in 4 ml of deionized water or isopropyl alcohol.

3. Results and discussion

3.1. Co_3O_4 nanoparticles

Figure 2 shows the results obtained from the characterization by Raman spectroscopy and TEM of the sample obtained using deionized water as the liquid medium. The Raman spectrum [Fig. 2a)] shows bands at 192, 480, 618, and 689 cm^{-1}.

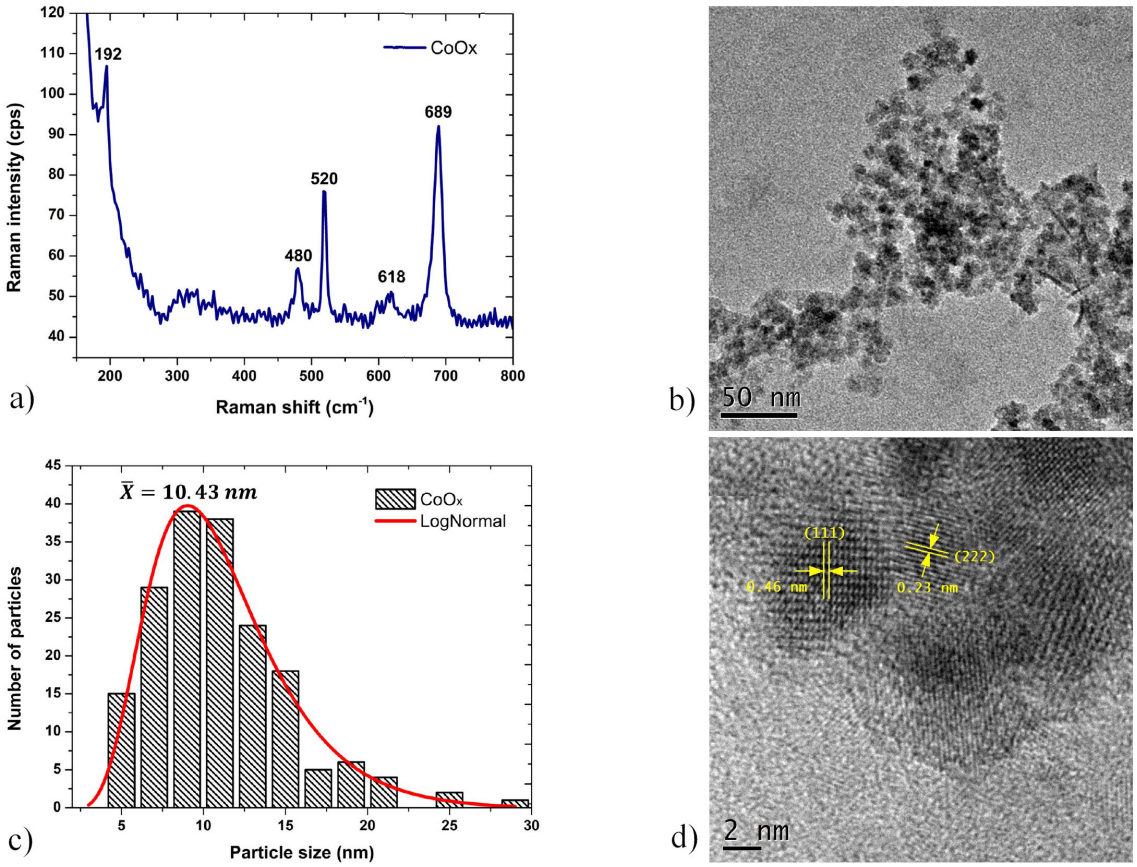

FIGURE 2. a) Raman spectrum, b) low-magnification TEM image, c) size distribution histogram, and d) high-resolution image of the sample obtained using deionized water as the liquid medium.

The bands found correspond to the Co_3O_4 phase of cobalt oxide [22,23]. In addition, a signal can be seen at 520 cm^{-1}, which corresponds to the silicon substrate on which the sample was placed for analysis.

Figure 2b) shows a low-magnification TEM image of the nanoparticles obtained, where it can be seen that the particles are partially agglomerated. Analysis of the size distribution [Fig. 2c)] indicates that the nanoparticles have an average diameter of 10.43 nm. Figure 2d) shows a high-resolution image (HRTEM) of the nanoparticles obtained, in which it is possible to see the planes associated with the cubic structure of the Co_3O_4 phase of cobalt oxide, such as the (111) plane, with an interplanar distance of 0.46 nm, and the (222) plane with an interplanar distance of 0.23 nm, which are approximate to those reported on the PDF-01-074-1657 chart for Co_3O_4.

These results indicate that under the ablation conditions described in the Experimental section and using deionized water as the liquid medium, only Co_3O_4 nanoparticles are obtained. This coincides with the findings reported by A. Rousta *et al.* [17] and E. N. Ghaem *et al.* [18], who also synthesized Co_3O_4 nanoparticles by ablating a cobalt target in deionized or distilled water. However, Rousta *et al.* report particle sizes close to 50 nm, which are larger than those obtained in this work. It is important to note that they used a higher laser fluence (100 J/cm^2), which increases the amount of ablated material and the energy transferred to the target, thus favoring the formation of larger particles.

3.2. CoOx/C nanomaterials

3.2.1. FTIR spectroscopy analysis

Figure 3a) shows the infrared spectrum of the sample obtained using the colloidal suspension of CNPs (CoOx/CNPs). For comparison purposes, the infrared spectrum of the liquid medium (CNPs) is included. The bands at 2957, 2924, 2858, 1460, and 1377 cm^{-1} are assigned to the stretching and bending vibrations of the C-H bonds in the CH_3 and CH_2 groups [24]. The signals at 1725 and 1250 cm^{-1} are due to the stretching of the C=O and C-O bonds [25]. The band at 1580 cm^{-1} is attributed to the bending of C=C bonds in aromatic rings [24]. The signal at 1120 cm^{-1} is assigned to the symmetric stretching of the C-O bonds in the C-O-C group [26]. The band at 1070 cm^{-1} is assigned to the asymmetric stretching of C-O-C [25]. A broad, intense band is observed at 905 cm^{-1} associated with the bending vibration of C-H bonds [26] or the asymmetric stretching vibration of Si-O bonds [27] in the substrate on which the sample was placed for analysis. Likewise, a signal was recorded at 1018 cm^{-1} due to the symmetric stretching of C-O-C [25]. And the signal at 740 cm^{-1} is due to the bending vibration of the C-H bonds [26]. In addition, for CoOx/CNPs we can observe a broad band at 3360 cm^{-1} which is due to the stretching vibration of the hydroxyl groups [24]. Furthermore, no signals associated with Co bonds were observed, which are present in the range of 576 to 661 cm^{-1} corresponding to metal-oxygen (Co-O) vibration modes [28].

Figure 3b) shows the infrared spectra of the sample obtained using the colloidal suspension of GONs (CoOx/GONs) and the liquid medium used during ablation (GONs). For CoOx/GONs, a broad band around 3260 cm^{-1} can be observed, which is due to the stretching vibration of the hydroxyl groups. The signal at 1595 cm^{-1} attributed to the asymmetric stretching of C=C bonds undergoes a slight shift towards 1572 cm^{-1} after the ablation process. In addition, we can see bands at 1373, 1010, and 1033 cm^{-1} associated with the vibrations of the C-H bonds and the stretching of the C-O bonds, respectively. Additionally, it is observed that the signal at 1705 cm^{-1}, corresponding to the vibrations of the C=O bonds, disappears completely after ablation. This behavior suggests a reduction process of the material. Given that CoOx particles are generated directly in a liquid medium of graphene oxide nanosheets, it is reasonable to assume that the laser beam interacts with them, removing part of the oxygenated functional groups and thus promoting their reduction

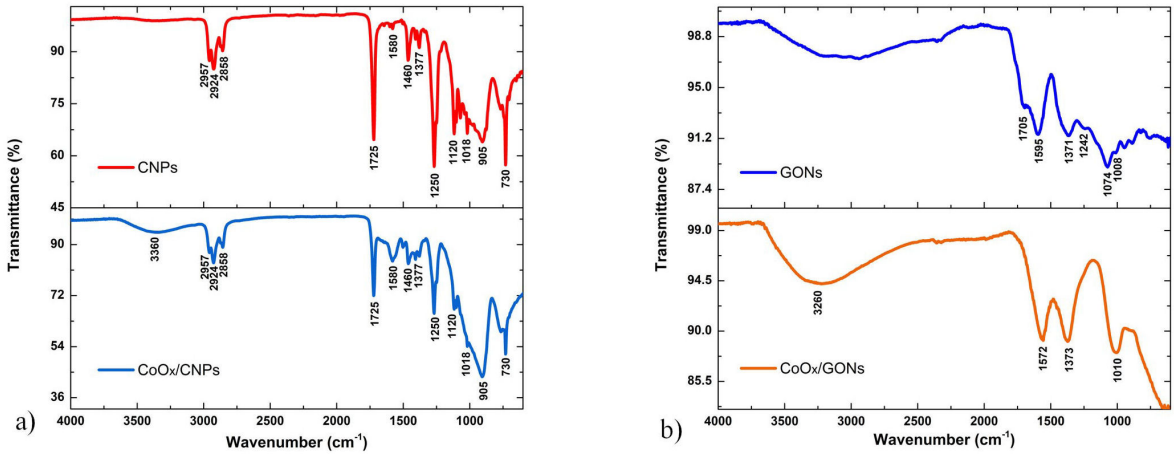

FIGURE 3. Infrared spectra of samples obtained using a) colloidal suspension of CNPs and b) colloidal suspension of GONs as the liquid medium, respectively.

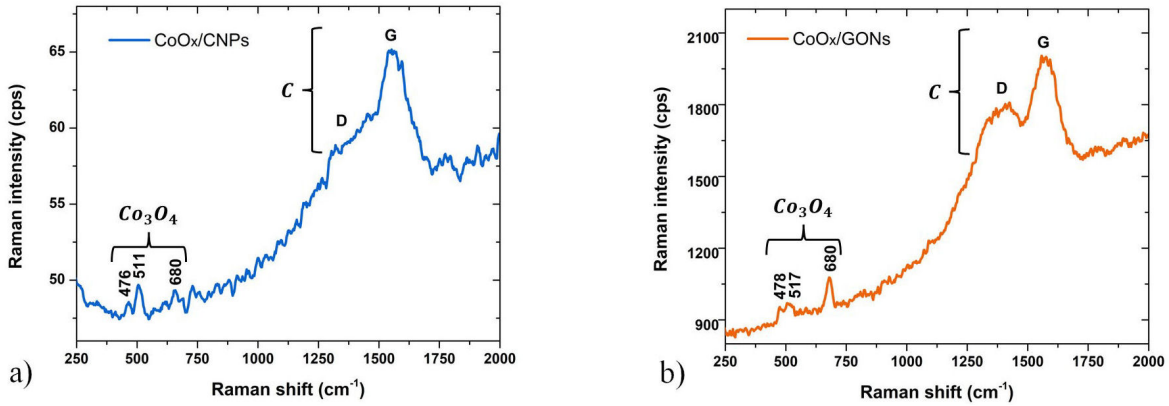

FIGURE 4. Raman spectra of samples obtained using a) colloidal suspension of CNPs and b) colloidal suspension of GONs as the liquid medium, respectively.

[29,30]. As in the previous case, it is not possible to observe signals associated with Co-O bonds.

3.2.2. *Raman spectroscopy analysis*

Figure 4 shows the Raman spectra of the materials obtained using the colloidal suspension of CNPs [Fig. 4a)] and the colloidal suspension of GONs [Fig. 4b)] as liquid media during the laser ablation process.

In the Raman spectrum for CoOx/CNPs, the D band at 1360 cm^{-1} and the G band at 1560 cm^{-1} can be observed due to the presence of the carbon material used during synthesis, as well as weak signals around 476, 511, and 680 cm^{-1}, which are attributed to the presence of Co_3O_4. For CoOx/GONs, the D band at 1366 cm^{-1} and the G band at 1573 cm^{-1} can be seen, confirming the presence of the carbon material used during synthesis. Additionally, we have bands at 478, 517, and 680 cm^{-1}, which correspond to the Co_3O_4 phase of cobalt oxide.

The ratio between the intensities of the D and G bands (I_D/I_G) in carbon materials is related to the degree of structural disorder; the higher the I_D/I_G value, the more structural defects the sample contains and the lower the degree of order [31]. For the CoOx/CNPs sample, we have I_D/I_G = 0.56, while for the CoOx/GONs sample, we have $I_D/I_G = 0.90$, which is greater than for the material obtained with the colloidal suspension of CNPs, indicating a higher degree of structural disorder.

3.2.3. *TEM analysis*

Figure 5 shows TEM images for the sample obtained with the colloidal suspension of CNPs (CoOx/CNPs). Figure 5a) shows spherical nanoparticles, and the size histogram [Fig. 5b)] indicates that the particles have an average size of 13.06 nm. The image inserted in Fig. 5c) shows a spherical particle coated with a carbon layer approximately 13 nm thick. In the HRTEM image, it is possible to see in greater detail that the layer surrounding the particle is composed of a series of planes, with a separation between layers of approximately 0.35 nm, which is close to the separation between graphite layers [32]. Selected area electron diffraction (SAED) analysis reveals the formation of a ring pattern [Fig. 5d)], indicating that the sample obtained is polycrystalline. We have a ring that can be assigned to the (511) plane of the Co_3O_4 phase of cobalt oxide, a ring assigned to the (200) plane of metallic cobalt, and a ring assigned to the (100) plane of graphitic carbon or the (200) plane of the CoO phase of cobalt oxide, according to the information in cards PDF-01-074-1657, PDF-01-089-7093, PDF-00-008-0415, and PDF-01-074-2392.

In general, the use of organic solvents and alcohols during laser ablation synthesis leads to the formation of carbon-coated nanoparticles, as well as nanoparticles embedded in carbon matrices, and even the generation of carbides [33-36]. In this case, as already mentioned, carbon-coated CoOx nanoparticles were obtained. TEM analyses suggest the presence of Co_3O_4, CoO, and metallic cobalt nanoparticles; however, Raman spectroscopy only shows the presence of the Co_3O_4 phase. It is important to remember that Raman spectroscopy is a volumetric technique, while TEM provides localized information at the nanometer scale. Further analysis is needed to determine if it is possible to have any other phase of cobalt oxides.

On the other hand, the use of solvents with low oxygen content tends to decrease the degree of oxidation of nanoparticles generated by laser ablation. However, even HPLC-grade liquids may contain traces of atmospheric gases which can influence the ablation process [37]. In fact, several authors have reported that the presence of atmospheric gases can modify the synthesis of nanomaterials obtained by laser ablation [38,39]. Isopropyl alcohol can also act as an oxidizing agent, promoting the simultaneous formation of metal nanoparticles and metal oxides [40,41].

The formation process of CoOx/CNPs nanomaterials can be described as follows. During ablation, the energy from the laser pulses is transferred to the metal target, increasing its

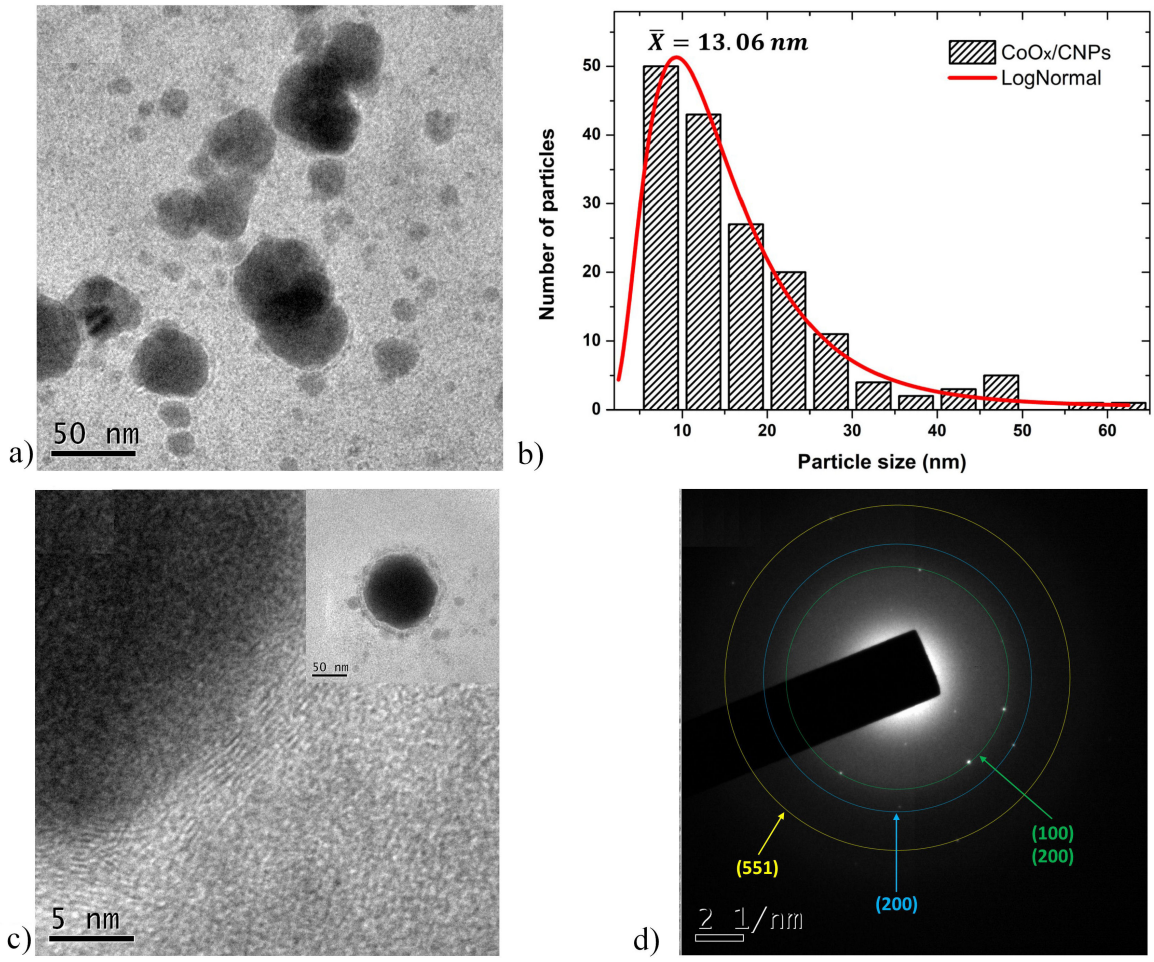

FIGURE 5. a) Low-magnification TEM image, b) size distribution histogram, c) low-magnification TEM image and HRTEM image showing a coated particle, and d) SAED pattern of nanomaterials obtained using the colloidal suspension of CNPs as the liquid medium.

temperature and generating a plasma plume composed of electrons, atoms, and cobalt ions. Similarly, part of the laser energy is distributed to the liquid medium-the colloidal suspension of CNPs in toluene/isopropyl alcohol-where the laser beam interacts with the CNPs and the solvent, causing their decomposition. This decomposition not only contributes carbon material to the nanomaterials formed, but also generates reactive species that, during the nucleation and growth of the nanoparticles, interact with the electrons, atoms, and ions from the cobalt target, promoting the formation of the different phases of cobalt oxide.

Figure 6a) shows a low-magnification image of the nanomaterials obtained using the colloidal suspension of GONs (CoOx/GONs). In it, spherical particles within a carbon matrix can be observed. The size histogram, Fig. 6b), indicates that the particles have an average size of 8.66 nm. Figure 6c) shows an HRTEM image of the nanoparticles obtained, in which it is possible to see the planes that make up the crystalline structure of the nanoparticles, such as the (100) plane with an interplanar distance of 0.21 nm corresponding to graphitic carbon [42]. SAED analysis reveals the formation of a ring pattern [Fig. 6d)] due to the (220) and (622) planes of the Co_3O_4 phase. We can also observe a ring that can be assigned to the (100) plane of graphitic carbon or the (200) plane of the CoO phase of cobalt oxide, according to the information in cards PDF-01-074-1657, PDF-01-074-2392, and PDF-00-008-0415.

When the colloidal suspension of GONs was used, spherical CoOx nanoparticles embedded in a carbon matrix were obtained. Similar to what was observed in the previous sample, TEM analyses indicate the presence of Co_3O_4 and CoO nanoparticles; however, Raman spectroscopy only detects signals corresponding to the Co_3O_4 phase. Therefore, complementary techniques are needed to better identify the phases present in the nanoparticles generated during the ablation process.

The mechanism of formation of these nanomaterials can be described as follows. As explained above, laser pulses

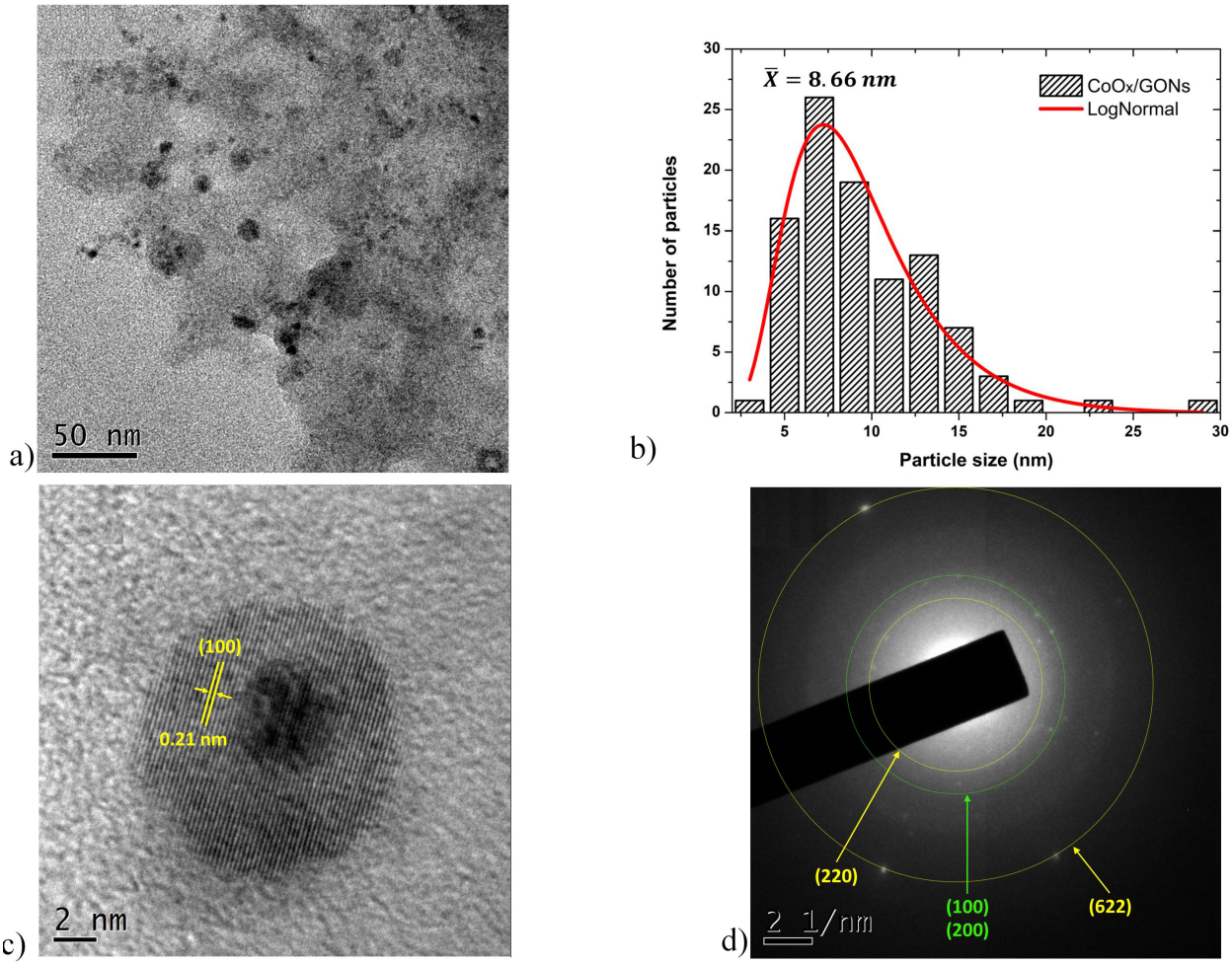

FIGURE 6. a) Low-magnification TEM image, b) size distribution histogram, c) HRTEM image, and d) SAED pattern of nanomaterials obtained using a colloidal suspension of GONs as the liquid medium.

produce a plasma plume composed of electrons, ions, and atoms released from the cobalt target, in addition to generating oxidizing species from the water in the liquid medium. The material ejected from the target reacts with these oxidizing species, giving rise to different phases of cobalt oxides. Subsequently, the nucleation and growth of nanoparticles begin, which become trapped and immobilized between the GONs [29,30].

Additionally, GONs can absorb part of the laser beam's energy, which promotes their deformation and the elimination of some oxygenated functional groups, resulting in their partial reduction. This energy absorption acts as a filter that limits the amount of energy arriving at the cobalt target, thus modifying the formation conditions and promoting the formation of a phase mixture. This occurs even when ablation experiments are performed for 30 min, which in laser ablation in water would be sufficient to obtain exclusively Co_3O_4 nanoparticles. Consequently, the effective energy reaching the target is not sufficient to stabilize a single metal oxide phase, or the early immobilization of the nanoparticles by graphene oxide prevents complete transformation to the Co_3O_4 phase.

These results indicate that when the ablation medium contains preformed carbon nanomaterials, it is possible to synthesize two types of structures: carbon-coated CoOx nanoparticles and spherical CoOx nanoparticles embedded in a carbon matrix. For example, A. G. Rad *et al.* [43] report the synthesis of cobalt oxide/graphene nanocomposites using a two-step process. In the first stage, a graphite target is irradiated in distilled water to generate graphene nanosheets; subsequently, this colloidal suspension is used as a liquid medium for the laser ablation of a cobalt target. This produces cobalt oxide nanoparticles with an average size of 25 nm deposited on the graphene nanosheets. Similarly, M. Khandelwal *et al.* [44] describe the production of graphene nanosheets decorated with Co_3O_4 nanoparticles using laser-assisted pyrolysis. These results, like those obtained in the present work, highlight the potential use of laser-assisted material synthesis and processing for the development of novel materials with diverse applications.

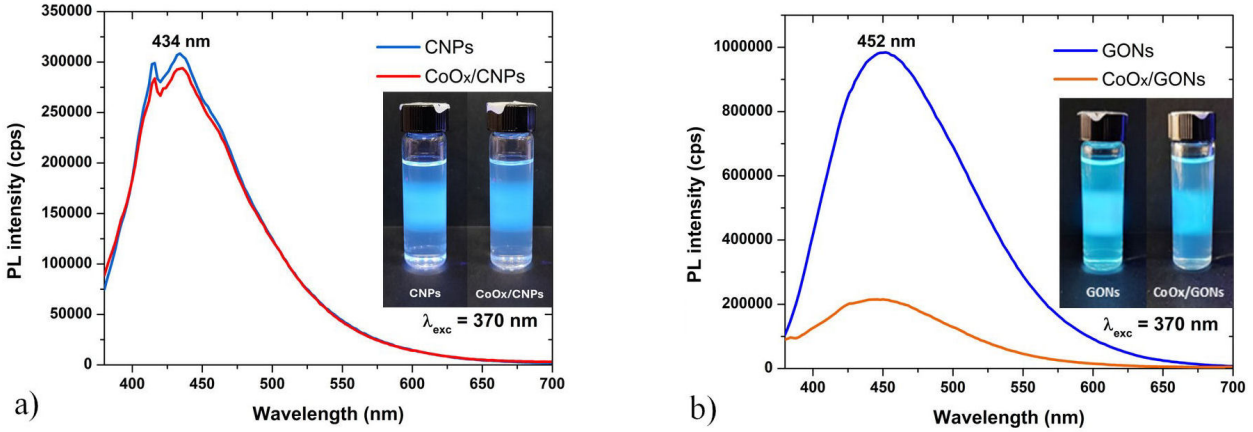

FIGURE 7. Photoluminescence emission spectra of samples obtained using a) colloidal suspension of CNPs and b) colloidal suspension of GONs as the liquid medium, respectively.

3.2.4. Fluorescence spectroscopy analysis

Figure 7 shows the photoluminescence emission spectra obtained at an excitation wavelength of 370 nm for the colloidal suspensions of CoOx/C nanomaterials (CoOx/CNPs and CoOx/GONs). The emission spectra of the liquid media used during the ablation process (CNPs and GONs) are also included for reference.

For the sample synthesized from the colloidal suspension of CNPs [Fig. 7a)], the incorporation of CoOx nanoparticles does not produce significant changes in the shape or position of the emission band (434 nm), compared to the liquid medium used during ablation. The inset in the figure shows a photograph of both suspensions under UV illumination ($\lambda = 370$ nm), where the beam path exhibits a blue hue in both cases. On the other hand, in the sample obtained from the colloidal suspension of GONs [Fig. 7b)], the position of the emission band (452 nm) remains virtually unchanged after the incorporation of CoOx. However, a decrease in photoluminescence intensity is observed compared to the liquid medium used during ablation. The corresponding insert again shows illumination under the UV lamp ($\lambda = 370$ nm), where the beam path is visible in blue-green tones.

Fluorescence intensity can decrease through various mechanisms, among which two widely studied quenching processes stand out: dynamic quenching, associated with collisions, and static quenching, related to the formation of complexes. Various substances can act as fluorescence inhibitors, including metal ions, which are capable of reducing photoluminescence in carbon nanomaterials. Previous studies have shown that incorporating these ions into carbon nanomaterials can decrease photoluminescence intensity. This is because metal ions can interact with functional groups present on the surface of the material, forming non-fluorescent complexes that enable new non-radiative deactivation pathways, ultimately leading to the extinction of photoluminescence [45,46]. In the case of CoOx/GONs, the infrared spectrum does not show the formation of new compounds; however, the disappearance of the band at 1705 cm^{-1} associated with C=O bond vibrations is observed. This suggests the partial elimination of some oxygen functional groups and, therefore, a slight reduction in graphene oxide after laser irradiation. This reduction could contribute to the observed loss of photoluminescence. However, to elucidate more precisely the mechanisms by which the incorporation of CoOx nanoparticles modifies the emission intensity, it will be necessary to use complementary techniques, such as time-resolved fluorescence spectroscopy.

4. Conclusions

The results obtained show that the solvent used during the synthesis of nanomaterials by laser ablation is an important parameter that significantly influences the composition and structure of the final products. When deionized water is used as the liquid medium, Co_3O_4 nanoparticles with an average diameter of 10.43 nm are formed. In contrast, the use of colloidal suspensions of carbon nanomaterials as the ablation medium leads to the formation of two types of CoOx/C nanomaterials: carbon-coated CoOx nanoparticles (CoOx/CNPs) and spherical CoOx nanoparticles embedded in a carbon matrix (CoOx/GONs). TEM analyses reveal the presence of Co_3O_4, CoO, and metallic cobalt nanoparticles; however, Raman spectroscopy only shows the presence of the Co_3O_4 phase. The use of complementary characterization techniques is therefore necessary to accurately identify the phases formed during the ablation of the cobalt target in colloidal suspensions of carbon nanomaterials. Furthermore, it was observed that in the case of CoOx/GONs, the incorporation of CoOx nanoparticles modifies the photoluminescent emission intensity of the colloidal suspension of GONs. This decrease in emission intensity could be associated with the reduction of graphene oxide by laser irradiation.

Acknowledgments

To Jorge Omar Esquivel and Dr. Oscar Olea for their support in the synthesis of materials by laser ablation. To Itzel Mi-

randa and Dr. Enrique Vigueras for the FTIR measurements. To Dr. Víctor H. Castrejón for his support in the acquisition of Raman spectra. To CONACyT for the 789629 postgraduate scholarship awarded to N. Enríquez-Sánchez.

1. S. Akram, M. ur Rahman, F. Maula, O. T. Satti, F. Ali, and I. L. Ikhioya, Enhanced Physical Properties of Cobalt Oxide Nanoparticles for Energy Storage Applications, *Nano-Horizons* **4** (2025) 17, https://doi.org/10.25159/3005-2602/16471
2. S. M. Ansari *et al.*, Cobalt nanoparticles for biomedical applications: Facile synthesis, physiochemical characterization, cytotoxicity behavior and biocompatibility, *Appl. Surf. Sci.* **414** (2017) 171, https://doi.org/10.1016/j.apsusc.2017.03.002
3. S. Iravani and R. S. Varma, Sustainable synthesis of cobalt and cobalt oxide nanoparticles and their catalytic and biomedical applications, *Green Chem.* **22** (2020) 2643, https://doi.org/10.1039/D0GC00885K
4. M. S. Muthu, P. Ajith, J. Agnes, M. Selvakumar, M. Presheth, and D. P. Anand, Hydrothermal synthesis and characterization of nano graphene oxide/cobalt oxide (GO/Co_3O_4) nanocomposite suitable for supercapacitor applications, *J. Mater. Sci.: Mater. Electron.* **34** (2023) 1766, https://doi.org/10.1007/s10854-023-11085-3
5. S. Zallouz, B. Réty, L. Vidal, J. M. Le Meins, and C. Matei Ghimbeu, Co_3O_4 nanoparticles embedded in mesoporous carbon for supercapacitor applications, *ACS Appl. Nano Mater.* **4** (2021) 5022, https://doi.org/10.1021/acsanm.1c00522
6. A. Mishra, A. Singh, H. R. Kushwaha, and A. Mishra, Cytotoxic effect of cobalt oxide-graphene oxide nanocomposites on melanoma cell line, *J. Exp. Nanosci.* **17** (2022), 509, https://doi.org/10.1080/17458080.2022.2115483
7. D. Zhang, Z. Li, and K. Sugioka, Laser ablation in liquids for nanomaterial synthesis: diversities of targets and liquids, *J. Phys. Photonics* **3** (2021) 042002, https://doi.org/10.1088/2515-7647/ac0bfd
8. V. Coviello, D. Forrer, P. Canton, and V. Amendola, Physical and chemical parameters determining the formation of gold-sp metal (Al, Ga, In, and Pb) nanoalloys, *Nanoscale* **16** (2024) 4745, https://doi.org/10.1039/D3NR04750D
9. A. De Bonis, M. Curcio, A. Santagata, and A. Galasso, and R. Teghil, Transition Metal Carbide Core/Shell Nanoparticles by Ultra-Short Laser Ablation in Liquid, *Nanomaterials* **10** (2020) 145, https://doi.org/10.3390/nano10010145
10. M. K. Ahmed, M. E. El-Naggar, A. Aldalbahi, M. H. El-Newehy, and A. A. Menazea, Methylene blue degradation under visible light of metallic nanoparticles scattered into graphene oxide using laser ablation technique in aqueous solutions, *J. Mol. Liq.* **315** (2020) 113794, https://doi.org/10.1016/j.molliq.2020.113794
11. N. Enríquez-Sánchez, A. R. Vilchis-Nestor, S. Camacho-López, M. A. Camacho-López, and M. Camacho-López, Colloidal MnOx NPs/Carbon sheets nanocomposite synthesis by laser ablation in liquids, *Opt. Laser Technol.* **146** (2022) 107591, https://doi.org/10.1016/j.optlastec.2021.107591
12. T. Tsuji, T. Hamagami, T. Kawamura, J. Yamaki, and M. Tsuji, Laser ablation of cobalt and cobalt oxides in liquids: influence of solvent on composition of prepared nanoparticles, *Appl. Surf. Sci.* **243** (2005) 214, https://doi.org/10.1016/j.apsusc.2004.09.065
13. J. D. Blakemore, H. B. Gray, J. R. Winkler, and A. M. Muller, Co_3O_4 nanoparticle water-oxidation catalysts made by pulsed-laser ablation in liquids, *ACS Catal.* **3** (2013) 2497, https://doi.org/10.1021/cs400639b
14. Y. Zhou, C. K. Dong, L. L. Han, J. Yang, and X. W. Du, Top-down preparation of active cobalt oxide catalyst, *ACS Catal.* **6** (2016) 6699, https://doi.org/10.1021/acscatal.6b02416
15. H. Wan *et al.*,, Improved lithium storage properties of Co_3O_4 nanoparticles via laser irradiation treatment, *Electrochim. Acta* **281** (2018) 31, https://doi.org/10.1016/j.electacta.2018.05.156
16. S. S. Kanakkillam, B. Krishnan, D. Avellaneda, and S. Shaji, Surfactant free stable cobalt oxide nanocolloid in water by pulsed laser fragmentation and its thin films for visible light photocatalysis, *Colloids Surf. A* **594** (2020) 124657, https://doi.org/10.1016/j.colsurfa.2020.124657
17. A. Rousta, D. Dorranian, and M. Elahi, Electrophoretic deposition of cobalt oxide nanoparticles on aluminium substrate, *Surf. Eng.* **36** (2020) 919, https://doi.org/10.1080/02670844.2019.16898
18. E. N. Ghaem, D. Dorranian, and A. H. Sari, Characterization of cobalt oxide nanoparticles produced by laser ablation method: Effects of laser fluence, *Physica E Low Dimens. Syst. Nanostruct.* **115** (2020) 113670, https://doi.org/10.1016/j.physe.2019.113670
19. H. Kwong, M. Wong, C. W. Leung, Y. Wong, and K. Wong, Formation of core/shell structured cobalt/carbon nanoparticles by pulsed laser ablation in toluene, *J. Appl. Phys.* **108** (2010) 034304, https://doi.org/10.1063/1.3457216
20. H. Zhang, C. Liang, J. Liu, Z. Tian, and G. Shao, The formation of onion-like carbon-encapsulated cobalt carbide core/shell nanoparticles by the laser ablation of metallic cobalt in acetone, *Carbon* **55** (2013) 108, https://doi.org/10.1016/j.carbon.2012.12.015
21. N. Enríquez-Sánchez, A. R. Vilchis-Nestor, M. A. Camacho-López, N. Zamora-Romero, S. Camacho-López, and M. Camacho-López, Synthesis and characterization of photoluminescent colloidal suspensions of carbon nanomaterials obtained from ultrasound irradiation of coffee waste in different solvents, *Diam. Relat. Mater.* **161** (2026) 113161, https://doi.org/10.1016/j.diamond.2025.113161
22. A. Numan *et al.*, Facile sonochemical synthesis of 2D porous Co_3O_4 nanoflake for supercapattery, *J. Alloys Compd.*

819 (2020) 153019, https://doi.org/10.1016/j.jallcom.2019.153019

23. J. Singh *et al.*, Effect of calcination temperature on structural, optical and antibacterial properties of ball mill synthesized Co_3O_4 nanomaterials, *J. Mater. Sci: Mater Electron.* **33** (2022) 3250, https://doi.org/10.1007/s10854-021-07526-6
24. A. J. García-Salcedo, L. A. Giraldo-Pinto, D. J. Márquez-Castro, and L. Tirado-Mejía, Influence of synthesis parameters on the optical properties of carbon dots, *Carbon Trends* **17** (2024) 100403, https://doi.org/10.1016/j.cartre.2024.100403
25. H. Nie *et al.*, Carbon dots with continuously tunable full-color emission and their application in ratiometric pH sensing, *Chem. Mater.* **26** (2014) 3104, https://doi.org/10.1021/cm5003669
26. J. Lee, K.H. Kim, and E.E. Kwon, Biochar as a catalyst, *Renew. Sust. Energ. Rev.* **77** (2017) 70, https://doi.org/10.1016/j.rser.2017.04.002
27. C. Cano-Trujillo, C. García-Ruiz, F. E. Ortega-Ojeda, and G. Montalvo, Differentiation of blood and environmental interfering stains on substrates by Chemometrics-Assisted ATR FTIR spectroscopy, *Spectrochim. Acta A Mol. Biomol. Spectrosc.* **292** (2023) 122409, https://doi.org/10.1016/j.saa.2023.122409
28. A. S. Adekunle *et al.*, Potential of cobalt and cobalt oxide nanoparticles as nanocatalyst towards dyes degradation in wastewater, *Nano-Struct. Nano-Objects* **21** (2020) 100405, https://doi.org/10.1016/j.nanoso.2019.100405
29. P. Nancy, A. K. Nair, R. Antoine, S. Thomas, and N. Kalarikkal, In situ decoration of gold nanoparticles on graphene oxide via nanosecond laser ablation for remarkable chemical sensing and catalysis, *Nanomaterials* **9** (2019) 1201, https://doi.org/10.3390/nano9091201
30. R. Torres-Mendieta, D. Ventura-Espinosa, S. Sabater, J. Lancis, G. Mínguez-Vega, and J. A. Mata, In situ decoration of graphene sheets with gold nanoparticles synthetized by pulsed laser ablation in liquids, *Sci. Rep.* **6** (2016) 30478, https://doi.org/10.1038/srep30478
31. C. C. Zhang, S. Hartlaub, I. Petrovic, and B. Yilmaz, Raman Spectroscopy Characterization of Amorphous Coke Generated in Industrial Processes, *ACS Omega* **7** (2022) 2565, https://doi.org/10.1021/acsomega.1c03456
32. A. Vittore, M. R. Acocella, and G. Guerra, Edge-oxidation of graphites by hydrogen peroxide, *Langmuir* **35** (2019) 2244, https://doi.org/10.1021/acs.langmuir.8b03489.
33. D. Reyes-Contreras, M. A. González-Aguilar, M. A. Camacho-López, E. Vigueras-Santiago, and M. Camacho-López, Photoluminescent colloidal Cu@C-NPs suspensions synthesized by LASL, *Opt. Laser Technol.* **90** (2017) 102-108, https://doi.org/10.1016/j.optlastec.2016.11.004
34. M. Madrigal-Camacho, A. R. Vilchis-Nestor, M. Camacho-López, and M. A. Camacho-López, Synthesis of MoC@Graphite NPs by short and ultrashort pulses laser ablation in toluene under N_2 atmosphere, *Diam. Relat. Mater.* **82** (2018) 63, https://doi.org/10.1016/j.diamond.2017.12.019
35. D. Zhang, C. Zhang, J. Liu, Q. Chen, X. Zhu, and C. Liang, Carbon-Encapsulated Metal/Metal Carbide/Metal Oxide Core-shell Nanostructures Generated by Laser Ablation of Metals in Organic Solvents, *ACS Appl. Nano Mater.* **2** (2019) 28-39, https://doi.org/10.1021/acsanm.8b01541
36. M. Curcio, A. De Bonis, A. Santagata, A. Galasso, and R. Teghil, Effect of laser pulse duration on properties of metal and metal carbide nanoparticles obtained by laser in liquid synthesis, *Opt. Laser Technol.* **138** (2021) 106916, https://doi.org/10.1016/j.optlastec.2021.106916
37. V. Amendola, and M. Meneghetti, What controls the composition and the structure of nanomaterials generated by laser ablation in liquid solution?, *Phys. Chem. Chem. Phys.* **15** (2013), 3027, https://doi.org/10.1039/C2CP42895D
38. N. Luo, X. Tian, J. Xiao, W. Hu, C. Yang, L. Li, and D. Chen, High longitudinal relaxivity of ultra-small gadolinium oxide prepared by microsecond laser ablation in diethylene glycol, *J. Appl. Phys.* **113** (2013), 164306, https://doi.org/10.1063/1.4803035
39. M. Flores-Castañeda, and S. Camacho-Lopez, Si nanoparticle decorated $Bi_2O_2CO_3$ 2D nanocomposite synthesized by femtosecond laser ablation of solids in liquids and aging, *Opt. Laser Technol.* **158** (2023) 108891, https://doi.org/10.1016/j.optlastec.2022.108891
40. E. Giorgetti *et al.*, Preparation of small size nanoparticles by picosecond laser ablation and control of metal concentration in the colloid, *J. Colloid Interface Sci.* **442** (2015) 89, https://doi.org/10.1016/j.jcis.2014.11.066
41. P. K. Baruah, A. K. Sharma, and A. Khare, Role of confining liquids on the properties of $CuCu_2O$ nanoparticles synthesized by pulsed laser ablation and a correlative ablation study of the target surface, *RSC Adv.* **9** (2019) 15124, https://doi.org/10.1039/C9RA00197B
42. G. K. Yogesh, E. P. Shuaib, P. Roopmani, M. B. Gumpu, U. M. Krishnan, and D. Sastikumar, Synthesis, characterization and bioimaging application of laser-ablated graphene-oxide nanoparticles (nGOs), *Diam. Relat. Mater.* **104** (2020) 107733, https://doi.org/10.1016/j.diamond.2020.107733
43. A. G. Rad, E. Darabi, and A. K. Manea, Synthesis of graphene/cobalt oxide nanocomposite by pulsed laser ablation in water and its characteristics, *J. Theor. Appl. Phys.* **18** (2024) 182428, https://doi.org/10.57647/j.jtap.2024.1802.28
44. M. Khandelwal, A. P. Nguyen, C. V. Trana, and J. B. Inn, Simple fabrication of Co_3O_4 nanoparticles on N-doped laser-induced graphene for high-performance supercapacitors, *RSC Adv.* **11** (2021) 38547, https://doi.org/10.1039/D1RA08048B
45. D. Y. Wang *et al.*, Photoluminescence quenching of graphene oxide by metal ions in aqueous media, *Carbon* **82** (2015) 24, https://doi.org/10.1016/j.carbon.2014.10.017
46. L. Zhao *et al.*, Microwave-assisted facile synthesis of polymer dots as a fluorescent probe for detection of cobalt(II) and manganese(II), *Anal. Bioanal. Chem.* **411** (2019) 2373, https://doi.org/10.1007/s00216-019-01678-5